



Article

Analysis of the Driving Mechanism of Grassland Degradation in Inner Mongolia Grassland from 2015 to 2020 Using Interpretable Machine Learning Methods

Zuopei Zhang 1,2, Yunfeng Hu 1,2,* and Batunacun 3 a

- State Key Laboratory of Resources and Environmental Information System, Institute of Geographic Sciences and Natural Resources Research, Chinese Academy of Sciences, Beijing 100101, China; zhangzuopei19@mails.ucas.ac.cn
- College of Resources and Environment, University of Chinese Academy of Sciences, Beijing 100049, China
- ³ College of Geographical Science, Inner Mongolia Normal University, Hohhot 010028, China; batunacun@imnu.edu.cn
- * Correspondence: huyf@lreis.ac.cn

Abstract: In traditional studies on grassland degradation drivers, researchers often lacked the flexibility to selectively consider driving factors and quantitatively depict their contributions. Interpretable machine learning offers a solution to these challenges. This study focuses on Inner Mongolia, China, incorporating four categories and sixteen specific driving factors, and employing four machine learning techniques (Logistic Regression, Random Forest, XGBoost, and LightGBM) to investigate regional grassland changes. Using the SHAP approach, contributions of driving factors were quantitatively analyzed. The findings reveal the following: (1) Between 2015 and 2020, Inner Mongolia experienced significant grassland degradation, with an affected area reaching 12.12 thousand square kilometers. (2) Among the machine learning models tested, the LightGBM model exhibited superior prediction accuracy (0.89), capability (0.9), and stability (0.76). (3) Key factors driving grassland changes in Inner Mongolia include variations in rural population, livestock numbers, average temperatures during the growth season, peak temperatures, and proximity to roads. (4) In eastern and western Inner Mongolia, changes in rural population (31.4%) are the primary degradation drivers; in the central region, livestock number changes (41.1%) dominate; and in the southeast, climate changes (19.3%) are paramount. This work exemplifies the robust utility of interpretable machine learning in predicting grassland degradation and offers insights for policymakers and similar ecological regions.

Keywords: machine learning; grassland degradation; driving factors; SHAP method; climate change



Academic Editor: Mark Altaweel

Received: 25 December 2024 Revised: 7 February 2025 Accepted: 11 February 2025 Published: 12 February 2025

Citation: Zhang, Z.; Hu, Y.; Batunacun. Analysis of the Driving Mechanism of Grassland Degradation in Inner Mongolia Grassland from 2015 to 2020 Using Interpretable Machine Learning Methods. *Land* 2025, 14,386. https://doi.org/10.3390/ land14020386

Copyright: © 2025 by the authors. Licensee MDPI, Basel, Switzerland. This article is an open access article distributed under the terms and conditions of the Creative Commons Attribution (CC BY) license (https://creativecommons.org/licenses/by/4.0/).

1. Introduction

Grasslands represent the largest ecosystem type in terms of terrestrial surface area, covering 37% of the global land area [1]. Over the past two decades, approximately 50% of global grasslands have experienced degradation, with 5% undergoing severe degradation [2]. In China, degraded grasslands have reached an area of 86.67×10^4 km² [3], which constitutes about 22.7% of China's total grassland area [4]. However, some studies have also shown that, against the background of the overall degradation of grasslands in China, the vegetation cover in some parts of China has been increasing, contributing to 25% of the global increase in leaf area index [5]. Grassland degradation reduces vegetation cover, leading to decreased grassland productivity, loss of biodiversity, and reduced species

Land 2025, 14, 386 2 of 19

richness; at the same time, grassland degradation also has a great impact on soil nutrient status, water content capacity, and soil structure [6–8]. Conversely, the improvement of grassland vegetation structure and cover is conducive to the improvement and enhancement of grassland ecosystem services, thus supporting the sustainability of the regional ecological–economic system. In conclusion, grassland changes can have a significant impact on the structure, function and service level of the ecosystem, and the sustainable development of the regional economy and society [9–11].

In order to analyze the temporal and spatial processes of grassland evolution, researchers use a series of satellite remote sensing parameter indicators for monitoring [12–14]. These indicators include net primary production (NPP), normalized difference vegetation index (NDVI), fractional vegetation cover (FVC), above-ground biomass (AGB), and so on. These indicators can reflect the status of grassland ecosystems from different dimensions, such as photosynthetic activity of grassland, vegetation growth and carbon storage of ecosystems, and other characteristics. In particular, NPP, as an indicator of grassland ecosystems, reflects key attributes such as vegetation cover, height, and photosynthetic capacity, offering insights into the overall status of grassland ecosystems, though it does not fully capture all of their multidimensional characteristics [15–17]. The analysis of grassland NPP change and its influencing elements can portray the evolution of the grassland ecosystem and reveal the driving elements of grassland evolution. Therefore, the exploration of the trend of grassland NPP change and its driving mechanism is the key to repairing and managing degraded grassland ecosystems, maintaining and improving the structure and service level of excellent grassland ecosystems, and promoting regional sustainable development.

In traditional studies targeting grassland NPP changes, researchers generally use ecological process simulation, dynamics simulation, and other methods to simulate the temporal-spatial change process of grassland NPP. For example, in ecosystem simulation (such as CASA model, GLOPEM model [18-20]), high temporal and spatial resolution and high precision estimation of NPP can be realized based on the vegetation growth mechanism combined with satellite remote sensing observation data. In the simulation of land change dynamics (such as CA-Markov model, FLUS model), the integrated effects of natural and human elements can be considered comprehensively, so as to realize the estimation of the changes in the NPP of the grassland on the basis of the dynamic simulation of land use [21,22]. Obviously, the above two methods can only simulate the temporalspatial changes of NPP based on the key elements (such as natural geographic and climatic factors) that have already been identified by the model and the quantitative relationship between the key elements and NPP. Researchers cannot introduce new key elements (such as economic activities), discover new patterns of NPP change by analyzing the relationship between key elements and NPP, and construct new simulation and prediction models. These shortcomings affect the comprehensiveness and effectiveness of the analysis of the grassland change driving mechanism. For this reason, some researchers have applied correlation analysis, regression analysis and residual analysis to explore the key driving factors driving grassland NPP and NDVI and their relative contributions [23–25]. Although these studies were able to freely select multiple driving factors and analyze the relationship between the driving factors and the changes of NPP and NDVI, the assumptions of correlation and regression analyses were too ideal, and it was difficult to simulate the nonlinear changes of NPP, and even more difficult to quantitatively give the contribution of each driving factor to the changes of NPP.

Machine learning (ML) methods provide a new possible way to overcome the above problems. In classical ML models, ML is increasingly used to recognize nonlinear relationships because the models do not require a priori expert knowledge and can extract patterns

Land 2025, 14, 386 3 of 19

and regularities directly from the data [26–28]. However, the shortcoming of classical ML models is that while ML relaxes the strict assumptions inherent in traditional models, it does so at the cost of not knowing the specific contributions of the parameters; the ML model becomes a "black box" [29]. Therefore, the development of explainable artificial intelligence (AI) has become the key to solving the problems of trust, transparency, causality, fairness, and visualization in classical AI models [30,31]. In this process, ML researchers have proposed the use of the SHAP (Shapely Additive Explanation) method to explain the results of ML, which has developed into explainable ML. For example, He et al. [32] used the Random Forest Model and SHAP method for quantitative precipitation estimation (QPE) based on satellite remote sensing, which provided an important basis for selecting input variables for satellite-based QPE. Li et al. [33] analyzed some key elements affecting the temporal and spatial variations of atmospheric particulate matter (PM_{2.5}) in Zhejiang Province, China, based on the Random Forest (RF) algorithm and the SHAP model, and found that the relative importance of industrial emissions decreased. To summarize, SHAP, as an ML model interpretation method, has been increasingly applied in the field of geoecology, but no exemplary application of the SHAP method in the analysis of the grassland change driving mechanism has been seen yet.

The factors driving grassland change are extremely complex and diverse. Researchers around the world have analyzed the variables that characterize grassland change at different spatial and temporal scales, and have conducted screening, correlation, and sensitivity analyses of the driving factors that drive those variables. These studies have laid the foundation for systematic and in-depth research on grassland change. For example, Lyu et al. [34] found that grazing exacerbated the degradation of grasslands in Xilinhot, while precipitation promoted the recovery of grasslands using the constraint line method. Zhou et al. [35] found that human activities and climate change were the main drivers of grassland degradation in China, with similar contribution rates. Zhao et al. [36] found that warm and wet climates increased diversity and warm and dry climates decreased diversity in Horqin, Inner Mongolia from 1992 to 2006, and that light grazing increased the richness and diversity of grasslands. Batunacun et al. [37] studied land degradation in Xilingol between 1975 and 2015 and found that the dominant elements driving land degradation change over time. In general, the main driving elements of grassland change may include various elements such as climate change, livestock structure, grazing intensity, grassland reclamation, urban development, tourism and settlement, transportation construction, and spatial relationships between elements. However, there are some problems in the existing studies, which are summarized as follows: the depth of the existing studies is not deep enough to trace the specific factors, and most of the studies fail to trace back to the specific and clear types of human activities and the time period of the activities; in terms of the selection of driving factors and the quantitative determination of the contribution rate of driving factors, there are also problems in the selection of driving factors, the doubtful applicability of the driving model, and the low degree of quantitative determination of the contribution rate.

To address the above issues, this study focuses on Inner Mongolia as the study area. It examines specific drivers of grassland change within the domains of geography, meteorology, ecology, and socioeconomic development. Multiple machine learning algorithms are applied to build a prediction model for NPP based on time-series data from 2015 to 2020. The study then compares and evaluates the performance of different ML methods in predicting grassland change. Finally, the SHAP method is used to interpret the ML results and identify key influencing factors. This study attempts to answer the following scientific questions:

Land 2025, 14, 386 4 of 19

1. What is the basic pattern of NPP change in Inner Mongolian grasslands from 2015 to 2020? What are the main driving factors and their contribution rates?

2. Which ML model performs best in predicting grassland NPP? How applicable is it?

2. Study Area and Data

2.1. Study Area

The Inner Mongolia Autonomous Region (Figure 1) is located in the north of China and is a typical distribution area of temperate steppe in Eurasia. The Inner Mongolia Autonomous Region extends from northeast to southwest; it is about 2400 km long from east to west and spans more than 1700 km from north to south, with a total land area of 1.183×10^6 square kilometers. The landform of the region is dominated by high plains, with mountainous hills such as the DaXingAnLing Mountains in the east. Most of the region is above 1000 m above sea level. As of February 2025, the Autonomous Region has nine prefecture-level cities and three leagues under its jurisdiction.

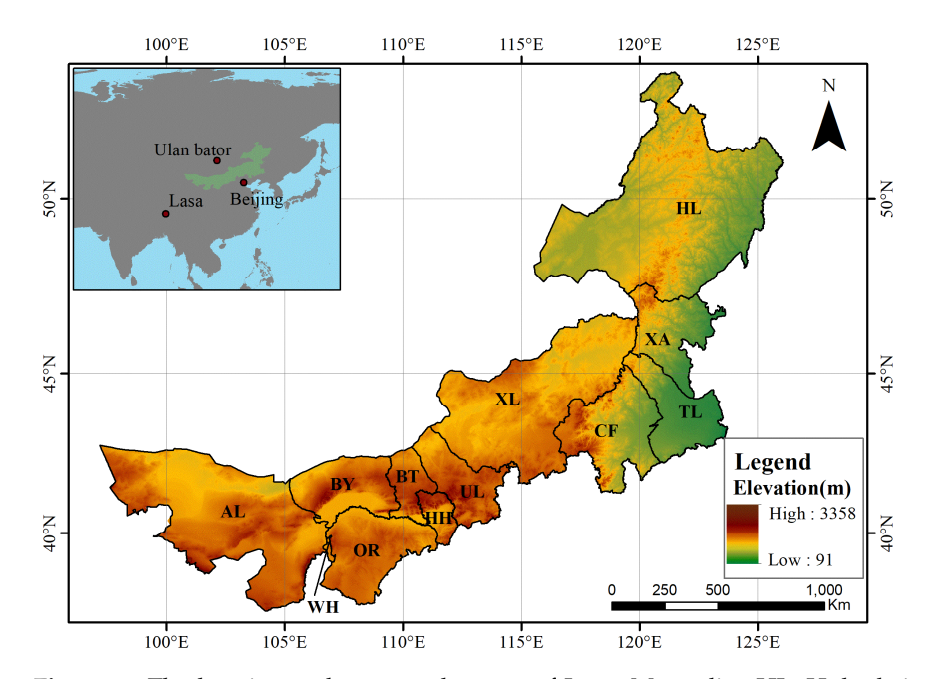


Figure 1. The location and topography map of Inner Mongolia. HL: Hulunbeier, XA: Xing'an, TL: Tongliao, CF: Chifeng, XL: Xilingol, UL: Ulanqab, BT: Baotou, HH: Hohhot, BY: Bayannur, OR: Ordos, WH: Wuhai, and AL: Alashan.

The study area has a typical mesothermal continental monsoon climate. From east to west, the climate zone gradually transitions from humid and semi-humid to semi-arid and arid. The average annual precipitation total for many years has been between 50 and 500 mm, and the annual rainfall gradually decreases from the southeast to the northwest. In summer, the average temperature of the whole region is around 25 °C; in winter, the lowest temperature in the central and western regions is below -20 °C, and the lowest temperature in the eastern regions is below -50 °C. Deciduous and coniferous forests are distributed in the northeast Daxinganling region, and deserts and bare rocky gravel lands with huge areas are distributed in the western Alxa League, Bayannur city and other regions; the southern edge of the region is an agricultural and pastoral transition zone, with cultivated land and grasslands distributed; the rest of the region is a type of grassland cover. From east to west, the grassland type gradually transitions from temperate meadow grassland and temperate typical grassland to temperate desert grassland, temperate desert steppe, and temperate desert and other zonal grassland types.

Land **2025**, 14, 386 5 of 19

2.2. Data Sets and Their Pre-Processing

NPP is used to characterize the status and quality of grassland ecosystems. The NPP data for 2015–2020 were obtained from the Terra Net Primary Production Gap-Filled Yearly Global 500m (MODIS/006/MOD17A3HGF) dataset [38]. The trend of NPP was used to characterize the improvement or degradation of grassland ecosystems: an increasing trend of NPP indicates improvement of grassland ecosystems; a decreasing trend of NPP indicates degradation of grassland ecosystems.

In order to analyze the driving mechanism of grassland change, four categories and sixteen specific elements, including geographical factors, meteorological factors, spatial factors and socioeconomic factors from 2015 to 2020, were selected in this study (Table 1). In particular, for geographic and spatial elements, we used their metrics (such as height and distance) to measure the magnitude of the driving force; for the two categories of elements, such as climate change and economic and social development, we used their trends (slope of change) during the period of 2015–2020 to measure the magnitude of the driving force.

Table 1. Driving factors and the response factor of the grassland.

Factors	Name	Definition/Content	Data Sources	
Response	NPP	Net primary production	MODIS/061/MOD17A3HGF (https://lpdaac.usgs.gov/products/mod1 7a3hgfv061/ (accessed on 20 January 2023))	
Coographical	Elevation	Height above sea level	SRTM Digital Elevation Data Version 4	
Geographical factors	Slope	Slope of terrain	(https://srtm.csi.cgiar.org/ (accessed on 15 January 2023))	
	AvgTMP	Average temperature of the growing season (May–September)	ECMWF/ERA5/MONTHLY https://cds.climate.copernicus.eu/cdsapp# !/dataset/reanalysis-era5-single-levels	
	MaxTMP	Maximum temperature of the growing season (May–September)		
	PDSI	Palmer drought severity index of the growing season (May–September)	(accessed on 14 February 2023)	
Meteorological factors	PREC	Average precipitation of the growing season (May–September)	IDAHO_EPSCOR/TERRACLIMATE	
	PET	Potential evapotranspiration of the growing season (May–September)	https://www.climatologylab.org/ terraclimate.html (accessed on 14 February 2023)	
	Soil_Mois	Soil moisture index of the growing season (May–September), derived using a one-dimensional soil water balance model		
	Dist_Water	Distance from a specific point to the nearest waterbody	OSM data	
	Dist_Rode	Distance from a specific point to the nearest road	https://www.openstreetmap.org/	
Spatial factors	Dist_Resid	Distance from a specific point to the nearest resident	Resource and Environmental Science and Data Centre, CAS http://www.resdc.cn (accessed on 5 March 2023)	
Socioeconomic factors	POP	Total population		
	Rural_POP GDP	Rural population Gross domestic production		
	GDP1	The primary industry, mainly referring to the agricultural industry in China.	Inner Mongolia Autonomous Region Bureau of Statistics	
	N_Herd	The number of main livestock in the Inner Mongolia region, including cattle, horses and	http://tj.nmg.gov.cn/ (accessed on 14 February 2023)	
	POP	sheep, is converted to standard sheep units. Total population		

Land 2025, 14, 386 6 of 19

(1) Geographical factors: DEM and slope. The DEM is NASA SRTM V3 data with a resolution of 30 m. With the support of the GEE platform, the NEAREST method was applied to resample the above index data and process them into raster files with 1 km resolution. On this basis, the terrain slope at 1 km resolution was calculated from the DEM.

- (2) Meteorological factors: six in total, all of which are relevant indicators for the growing season (May–September). They are precipitation (PREC), average temperature (AvgTMP), monthly maximum temperature (MaxTMP), potential evapotranspiration (PET), maximum drought index (PDSI), and average soil moisture (Soil_Mois). Among them, the temperature metrics were calculated from the monthly mean and maximum temperatures at 2 m above ground provided by the ERA5 dataset (ECMWF/ERA5/MONTHLY). Other indicators were calculated from the data provided by the Terraclimate dataset (IDAHO_EPSCOR/TERRACLIMATE). The above data were processed into 1 km resolution raster files with the support of the GEE platform.
- (3) Spatial factors: there are three in total, namely, distance from water bodies (Dist_Water), distance from roads (Dist_Road), and distance from settlements (Dist_Resid). The water body and road data were obtained from OSM data, and the settlement data were from the China Multi-Period Land Use Land Cover Remote Sensing Monitoring dataset (CNLUCC) provided by the Resource and Environment Data Center of the Institute of Geography, Chinese Academy of Sciences (http://www.resdc.cn). The shortest Euclidean distance from each point in space to the above points (settlement points) and lines (road and water body boundaries) was calculated by applying the Near method of ArcGIS at 1 km resolution.
- (4) Socioeconomic factors: five in total, namely, gross domestic product (GDP), primary industry output (GDP1), total population (POP), rural population (Rural_POP), and number of livestock (N_Herd) (including cattle, sheep, and horses, which are converted according to the standard to be expressed as a standard sheep unit).

Population density data were obtained from Worldpop data (https://hub.worldpop.org/ (accessed on 13 February 2023)) [39]. The data were spatialized from census data, combined with remote sensing imagery, applying the Random Forest method. GDP, gross primary industry product, rural population, and livestock data were obtained from year-book data provided by the Inner Mongolia Bureau of Statistics (http://tj.nmg.gov.cn/ (accessed on 18 December 2022)).

The Theil–Sen Median method is a robust nonparametric statistical method for trend calculation [40], which has the advantages of high computational efficiency and insensitivity to measurement errors and outlier data, and is suitable for trend analysis of time series data. Its formula is as follows:

$$\beta = Median\left(\frac{x_j - x_i}{j - i}\right) \quad \forall j > i \tag{1}$$

where Median() denotes to take the median value. x_j and x_i represent different years of data, respectively, and j and i are the year. If β is greater than or equal to 0, it indicates that the factor is increasing or unchanged, and if β is negative, it indicates that the predictor is decreasing. For Theil–Sen Median change analysis, it is necessary to apply the Mann–Kendall (MK) method to test the significance of the change. The Mann–Kendall (MK) test is a nonparametric test of trend in time series. The MK method does not require the measurements to follow a normal distribution, is unaffected by missing values and outliers, and is suitable for long time series data for trend significance testing.

Land 2025, 14, 386 7 of 19

When using the ML model to carry out the predictive analysis, the dataset training labels were denoted as 0 for image elements where the grassland was stable and unchanged or improved (i.e., unchanged or increased by the MK test of the NPP), and 1 for image elements where the grassland was degraded (i.e., declined by the MK test of the NPP). For the two types of elements such as climate change, economic and social development (i.e., AvgTemp, MaxTMP, PDSI, PREC, PET, Soil_Mois, GDP, GDP1, POP, Rural_POP, N_Herd, etc.) and changes in grassland ecological response factors (NPP), the authors applied the Theil–Sen Median method to calculate the 2015–2020, raster-point-by-point, changes in these elements (1 km²) change slopes.

Most of the above data processing was performed under Matlab 2021b support, and the training data extraction was carried out under ArcGIS 10.3.

3. Research Methods

3.1. Technology Route

The technical route of the study is shown in Figure 2.

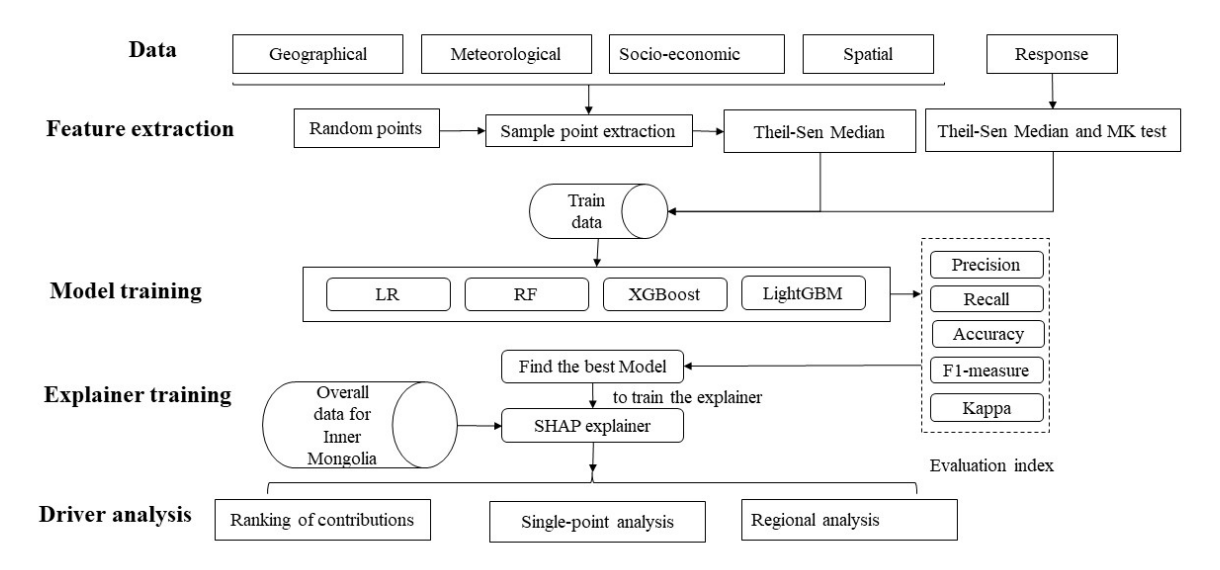


Figure 2. Workflow for the grassland change and its driving mechanism analysis.

First, 15,000 points were randomly generated within the study area with the support of the ArcGIS platform. From this, the values of NPP and other driving elements were extracted for these 15,000 points, from 2015 to 2020.

Then, out of the above 15,000 points, 75% (11,250 points) and 25% (3750 points) of them were used as training data and validation data, respectively. Four models, including LR, RF, XGBoost, and LightGBM, were selected to carry out the training and accuracy assessment of the ML models and to identify the best ML model for predicting the changes of NPP in Inner Mongolia grassland.

Then, using the best ML model identified in the previous step, the SHAP interpreter was applied to rank the importance of the driving factors driving grassland changes; analysis and spatial mapping were conducted at the image element scale as well as the regional scale for the driving and dominant factors driving grassland changes in the study area.

3.2. ML Models

A total of four ML methods are explored in this study, namely, Logistic Regression (LR), RF, XGBoost, and LightGBM.

Land 2025, 14, 386 8 of 19

LR is a linear method that is widely used to model land use and the analysis of the driving elements of land use change. The LG optimization parameters used in this study are enalty = "12", solver = "liblinear", C = 1, and max_iter = 1000.

Random Forest (RF) is an integrated learning algorithm based on decision trees proposed by Breiman [41], which improves classification accuracy by constructing multiple decision trees and synthesizing their predictions. Previous researchers have also carried out a lot of research work on the study of grassland degradation using Random Forests [42–44]. In this study, the RF model uses the following parameters: $n_estimators = 600$, $max_depth = 20$, $min_samples_leaf = 20$, $random_state = 10$, and $r_jobs = -1$.

The XGBoost algorithm is an algorithm based on Boosting idea and GBDT proposed by Chen and Guestrin [45]. The XGBoost algorithm limits overfitting, minimizes training losses, and reduces classification errors when developing the final model. For this study, the XGBClassifier used the following parameters: learning_rate = 0.1, ax_depth = 5, n_estimater = 300, min_child_weight = 3, and lambda = 10.

The LightGBM algorithm is an optimization model of XGBoost with improvements in information gain, decision tree construction, and feature parallelism. Compared to XGBoost, LightGBM occupies less memory in the operation and is relatively faster. In this study, the LightGBM classifier uses the following parameters: learning_rate = 0.1, num_leaves = 60, min_sum_hessian_in_leaf = 6, and lambda_l1 = 0.1.

All of the above modeling algorithms are carried out in the Python 3.7, Jupyter notebook platform and supported by XGBoost library, LightGBM library and Sklearn library. The above models, parameter schemes, basic data, and resultant data involved in this study have been uploaded to the Zenodo platform (https://zenodo.org/10.5281/zenodo.14833139). Readers can download and validate them by themselves.

3.3. Shapley Additive Explanations (SHAP) Analysis

Although most ML algorithms have a built-in feature importance ranking algorithm, this feature ranking algorithm only takes into account the influence of each predictor on the node splits or the predicted values and does not give a judgment on the positivity or negativity. Compared with feature importance, SHAP value makes up for this deficiency. The SHAP value not only gives the degree of importance of the variable, but also gives the positivity or negativity of the impact [46].

Specifically, the SHAP interpreter combines the values of each feature into a set of feature subsets and calculates the contribution of each feature subset to the model prediction results, thus obtaining a Shapley value for each feature. The SHAP value can be interpreted as the contribution of the feature to the model prediction results and can also be used to visualize and interpret the prediction results of an ML model. The mean of the absolute SHAP values for each feature over the overall sample represents the importance of that feature: the larger the mean SHAP value, the more important the feature is, and the larger the contribution of the change in feature value in driving the change in the dependent variable. In a SHAP plot, a Shapley value greater than 0 indicates that the factor has a positive contribution; a Shapley value less than 0 indicates that the factor has a negative contribution.

3.4. Validation of the Model

In the study, the authors used data from 11,250 points to carry out the training of the ML model and used data from another 3750 points as the accuracy validation dataset. The authors selected five metrics, precision, recall, accuracy, F1-measure, and Kappa coefficient, as the precision evaluation metrics of the model. Among them, precision, accuracy and F1-Score, reflect the accuracy of model prediction; recall reflects the predictive ability of

Land 2025, 14, 386 9 of 19

the model; and Kappa reflects the stability of the model. The above five indicators have been widely used in ML research, and this paper will not repeat the specific formula of each indicator [47].

4. Analysis of Results

4.1. Spatial Distribution Patterns of Grassland Change

The changing trend of grassland in Inner Mongolia is shown in Figure 3. In 2015, based on MODIS land cover data, the area of grassland in the study area was 6.897×10^5 square kilometers, accounting for 58.4% of the national land area of Inner Mongolia. From 2015 to 2020, the total area of grassland undergoing changes was about 4.384×10^5 square kilometers. Among them, the area of NPP increase (NPP increase and passed the significance test, NPP increase but did not pass the significance test) reached 3.171×10^5 square kilometers, and the area of NPP decrease (NPP decrease and passed the significance test, NPP decrease but did not pass the significance test) reached 1.212×10^5 square kilometers.

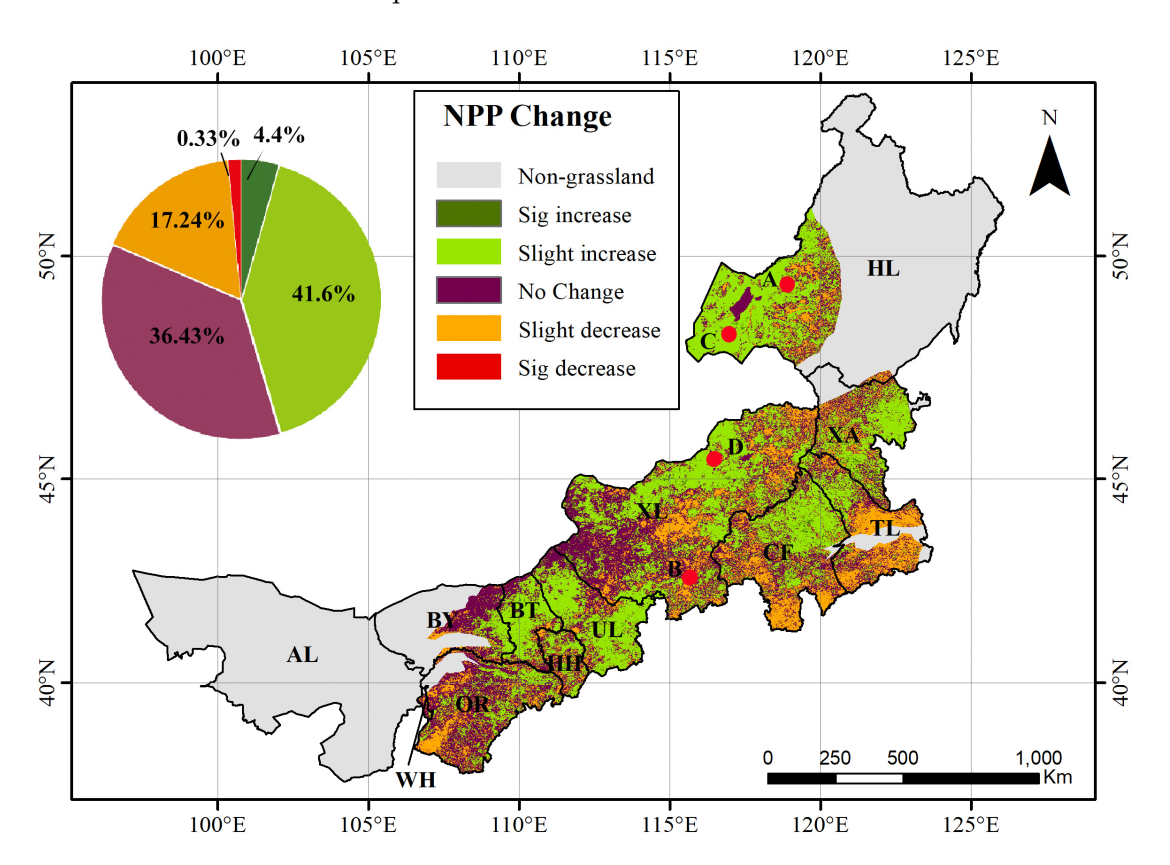


Figure 3. Change tendency of grassland NPP in Inner Mongolia from 2015 to 2020. Grassland areas with NPP change slope thresholds of 0–0.05 were designated as "No Changes" areas, and areas with NPP change slopes greater than 0.05 were designated as "Increase" areas; of these, areas that passed the MK significance test were designated as "Significant Increase" areas. Regions where the slope of NPP change is less than 0 are "Decrease" regions, and those that pass the MK significance test are "Significant Decrease" regions. Points A, B, C, D are four sampling sites for detail analyses in Section 4.4.

The NPP decrease in the eastern region is higher than that in the central and western regions, and the NPP decrease in the southern region is higher than that in the northern region. In terms of administrative regions, the more seriously degraded grassland areas are: Tongliao city, Chifeng city, Wuhai city, Ordos city and Hohhot city, and the proportion of NPP reduction to the grassland area in the respective administrative regions is 44.6%,

Land 2025, 14, 386 10 of 19

25%, 20.2%, 20.1%, and 17.6%, respectively. Grassland productivity improved in Ulanqab, Baotou, Hulunbeier, Xing'an, and Xilinguole; the proportions of the area with elevated grass NPP to the area of grassland in their respective administrative districts were 69%, 66.7%, 65.8%, 56.7%, and 43%, respectively.

4.2. Comparison of Prediction Accuracy of ML Models

Based on the accuracy validation on 3750 random sample points, the results of the accuracy assessment of the four models in three aspects, including model prediction accuracy, prediction ability and model stability, can be obtained (Table 2). The results show the following:

	Precision	Accuracy	F1-Score	Recall	Kappa		
LR	0.76	0.76	0.7	0.65	0.5		
XGBoost	0.85	0.86	0.84	0.86	0.71		
RF	0.85	0.87	0.84	0.83	0.72		
LightGBM	0.89	0.88	0.9	0.9	0.76		

Table 2. Predicting the effects comparison among four different ML models.

In the accuracy of model results (precision, accuracy and F1-Score), LightGBM has the best performance, followed by RF and XGBoost, and LR has the worst performance. In terms of model predictive power (Recall), LightGBM performs the best, followed by RF and XGBoost, and LR has the worst recall. In terms of model stability (Kappa), LightGBM and XGBoost models perform the best, followed by the RF model and the LR model is the worst. Taken together, LightGBM has higher prediction accuracy, prediction ability, and stability, as well as the advantages of a more concise structure and higher computational efficiency. Therefore, based on the current natural ecological environment of the study area and the model parameterization scheme, the LightGBM model becomes the best model for simulating and predicting NPP changes.

In the subsequent study, the authors use the SHAP method to carry out the analysis of the role mechanism and contribution rate of each factor to the LightGBM simulation results.

4.3. Driving Factors and Mechanism

Using the SHAP analysis method, the contribution of each factor in the LightGBM model results can be analyzed, which can be mapped out by the influencing factors and their degree of influence on all grass image elements in the study area, so as to obtain the ability of each parameter to influence the final results (Figure 4).

The vertical axis orders the features by the sum of the SHAP values of all samples. The closer to the top, the greater the influence of the feature on the NPP prediction. The horizontal axis is the distribution of SHAP values (the influence of the feature on the model output), which indicates the nature of the feature's influence and its magnitude; the right side (SHAP > 0) indicates that the feature has a positive influence on the prediction of the NPP change, which is a facilitating effect; the left side (SHAP < 0) indicates that the feature has a negative influence on the prediction of the NPP change, which is an inhibiting effect. Each point in the figure represents a sample, and the color of the point indicates the high or low value of the feature, with red corresponding to high values and blue corresponding to low values.

As seen in Figure 4, from top to bottom, changes in rural population size (Rural_POP), changes in livestock size (N_Herd), changes in average growing season temperature (AvgTMP), changes in maximum growing season temperature (MaxTMP), and distance to road (Dist_Road) are the most important elements influencing the degradation of NPP in Inner Mongolia during the period of 2015–2020.

Land 2025, 14, 386 11 of 19

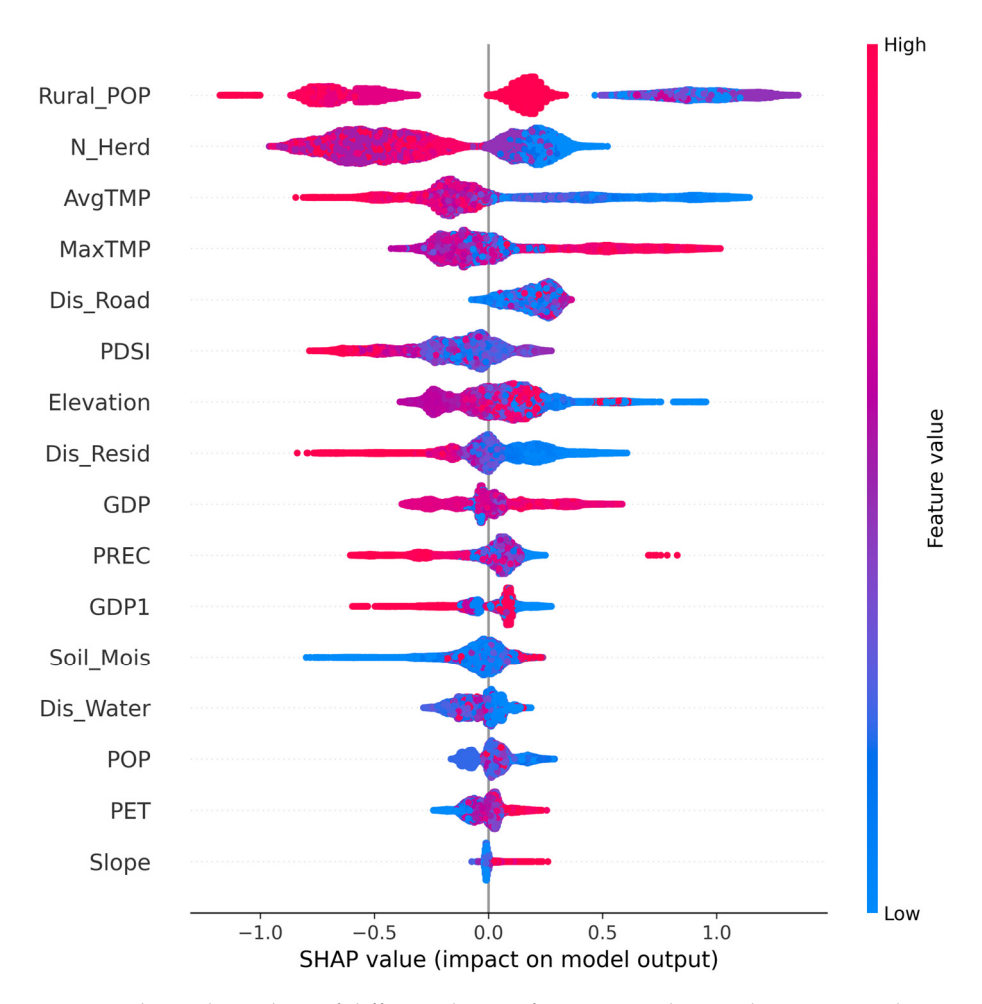


Figure 4. The ranking chart of different driving factors according to their SHAP values.

In terms of economic and social development, the majority of the region is characterized by an increase in rural population (red pixels), with a small number of areas experiencing a decrease in rural population (blue pixels); the region is characterized by an increase in the number of livestock (red pixels), with a small number of areas experiencing a decrease in the number of livestock (blue pixels). The figure shows that the increase in rural population and livestock number have an inhibiting effect on grassland degradation, while the decrease in rural population and livestock number have a promoting effect on grassland degradation. This result is not consistent with the general understanding. We hypothesize that the labor efficiency and output of farming is higher relative to the labor efficiency and output of livestock. As a result, the increased rural population, as well as part of the population previously engaged in animal husbandry, has mainly entered farming, which in turn has reduced the pressure on the grasslands from people's livelihood problems. On the other hand, the livestock populations of interest in this study include a wide range of livestock such as cattle, sheep, horses, etc., and changes in the populations of the different types of livestock may be of greater significance to changes in the quality of the grasslands.

In terms of regional climate change, most parts of the study area showed increased average growing season temperature (red pixels) and increased maximum growing season temperature (red pixels). An increase in the average growing season temperature (AvgTMP) inhibits grassland degradation, while an increase in the maximum growing season temperature (Max_TMP) promotes grassland degradation. An increase in AvgTMP usually means a longer growing season, which inhibits grassland degradation and is conducive to grassland improvement; whereas an increase in Max_TMP usually means the occur-

Land 2025, 14, 386 12 of 19

rence of extreme high temperatures, which can cause grassland drought, which causes grassland degradation.

In terms of spatial factor relationships, the presence of roads increases grassland degradation. The further away from the road (Dist_Road), the less prone to degradation, while the closer to the road (smaller Dist_Road), the more prone to degradation. This is related to the fact that pastoralists in the study area often graze along the narrow strip from the road to the pasture fence or migrate their livestock along that narrow strip.

4.4. Spatial Differences in Driving Mechanisms of Grassland Change

It is found that the driving mechanism of grassland change (key driving factors and their contribution rates) will be significantly different with the geographic location at the like metric scale (Figure 5). The four points located in Hulunbeier city and Xilingol League, respectively, (see Figure 3 for locations) are illustrated as follows:



Figure 5. Different driving mechanisms and contribution effects in different location. (**A**,**B**) are degraded grasslands in Xilingol and Hulunbeier, respectively; (**C**,**D**) are undegraded grasslands in Xilingol and Hulunbeier, respectively. Blue represents inhibition, red represents facilitation, and the length of the arrow represents the contribution.

At Point A, based on MODIS NPP time series data, it was shown that grassland degradation occurred when the NPP was $0.3351~{\rm kg\cdot C/m^2}$ in 2015 and decreased to $0.3183~{\rm kg\cdot C/m^2}$ in 2020. The driving mechanism analysis then showed that from 2015 to 2020, the decrease in rural population (-1.91), the decrease in average temperature (-0.2486), the distance from settlements ($1149.4829~{\rm m}$), the distance from roads ($9261.8618~{\rm m}$), the decrease in total population (-0.0204), and the elevation in GDP (0.12) were elements that had a grassland degradation promotion; the increase in livestock population (Theil–Sen fitted slope value of 0.1843) and specific altitude ($1029.0~{\rm m}$) were elements that had an inhibitory effect on grassland degradation. The combined effect resulted in an expected value of 0.64 for the probability of a decrease in NPP, i.e., grassland degradation; the predicted results were consistent with reality.

Land 2025, 14, 386 13 of 19

At Point B, based on MODIS NPP time series data, it is shown that grassland degradation occurs with an NPP of 0.2338 kg·C/m² in 2015 and 0.2227 kg·C/m² in 2020. The driving mechanism analysis, on the other hand, showed that from 2015 to 2020, the decreased rural population (-2.65), the distance from settlements (3146.0820 m), the distance from roads (7808.8143 m), the increased GDP (0.3), the altitude (1436 m), and the increased total population (0.421) were the elements that increased the expectation of grassland degradation, while the increased number of livestock (0.3037) and decreased PDSI (-0.104) decreased the expectation of grassland degradation. The combined effect results in an expected probability of 1.02 for a decrease in NPP, i.e., grassland degradation; the predicted results are consistent with reality.

At Point C, based on MODIS NPP time series data, it was shown that the NPP was $0.1832~{\rm kg\cdot C/m^2}$ in 2015 and $0.202~{\rm kg\cdot C/m^2}$ in 2020, and the grassland did not degrade, but rather improved. The analysis of driving mechanisms, on the other hand, showed that the decrease in average temperature (-0.3377), the distance from the settlement ($126.5657~{\rm m}$), the increase in GDP (0.5), and the decrease in the total population (-0.0827) in the period of 2015-2020 increased the expectation of degradation of the grassland, whereas the decreased rural population (-1.16), the increased number of livestock (0.9), and the altitude ($1022~{\rm m}$) were factors that decreased the expectation of grassland degradation. As a result of these factors, the expected value of the probability of a decrease in NPP reaches -0.99, i.e., no grassland degradation; the predicted results are consistent with reality.

At Point D, based on MODIS NPP time-series data, it was shown that the NPP was $0.1898~{\rm kg\cdot C/m^2}$ in 2015 and $0.2259~{\rm kg\cdot C/m^2}$ in 2020, and that the grassland was not degraded, but rather improved. The driving mechanism analysis, on the other hand, showed that from 2015 to 2020, the decrease in the average temperature during the growing period (-0.2744), the distance from the settlement ($553.1192~{\rm m}$), the altitude ($1332~{\rm m}$), and the increase in precipitation during the growing period (10.3333) were the elements that increased the expectation of the degradation of the grassland; whereas in regard to the decrease in the rural population (0-0.7857), the number of livestock (0.2296), increase in PDSI (0.113), and increase in GDP of the primary sector (0.6) are elements that decreased the expectation of grassland degradation. The combined effect of these elements results in an expected value of -1.04 for the probability of a decrease in NPP, i.e., no degradation of grassland; the predicted result is consistent with the reality.

4.5. Spatial Distribution of Dominant Factors of Grassland Degradation

Based on the SHAP values on each image element and each element in the study area, we extracted the element with the largest SHAP value (positive maximum value without considering the absolute value) on each image element, and thus we obtained the distribution map of the dominant elements of the degradation of Inner Mongolia grassland (Figure 6). The map only shows the elements with the largest driving effect on the image elements that have been in degradation, or those that may be in degradation.

In the vast majority of places, changes in the number of grassland livestock (including cattle, sheep, and horses) are the most important element driving grassland degradation. The total area of this image type amounted to $28.34~\rm km^2$, accounting for 41.1% of the total grassland area in the study area; it was concentrated in the central region of Inner Mongolia, including Xilingol League, Ulanqab city, Hohhot city, Baotou city, Bayannur city, and Ordos city.

Land 2025, 14, 386

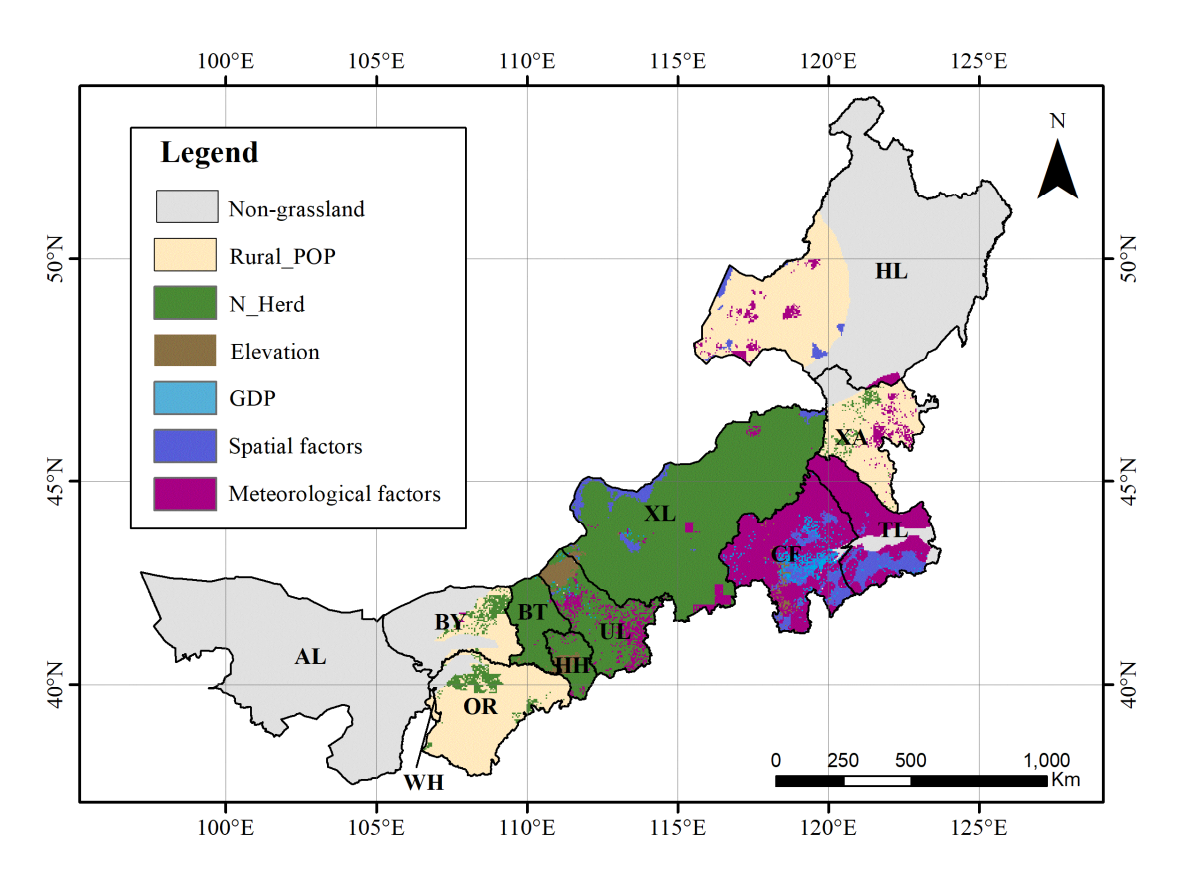


Figure 6. Dominant driving factor of grassland degradation in Inner Mongolia.

Rural population change is another important element driving grassland degradation in Inner Mongolia. The total area of this type of image element amounted to $21.66~\rm km^2$, accounting for 31.4% of the total area of grassland in the study area, and it was concentrated in the eastern region as well as the western region of Inner Mongolia, including Hulunbeier and Xing'an in the east, Ordos and Bayannur in the west, and other four allied cities.

Climate change, on the other hand, is also an important element driving grassland degradation in Inner Mongolia. The total area of this type of image element reaches 13.31 km², accounting for 19.3% of the total area of grassland in the study area, and it is concentrated in Tongliao and Chifeng in southeastern Inner Mongolia, with a small amount of distribution in the northwestern area of Xilingol.

Spatial relationship is the fourth major category of elements driving grassland degradation in Inner Mongolia. Among all the spatial relationship elements, distance from settlements as well as distance from roads had the greatest impact. The total area of these two categories of like elements was 3.45 km², accounting for 5% of the total grassland area in the study area. Moreover, the pixels affected by the settlement factor were mostly distributed in Hulunbeier city, and the pixels affected by the road factor were mostly distributed in Tongliao and part of Chifeng.

As for the terrain factor (elevation, slope), regional economy (GDP) and industrial development (primary industry) factors, it is very rare that they act as the dominant driving factors of grassland degradation in Inner Mongolia. The total area of these categories of like elements is only 1.17 km², accounting for less than 1.7% of the total grassland area.

5. Discussion

5.1. Spatial Variations and Policy Recommendations

The study showed that grassland degradation in Inner Mongolia is more serious in the north than in the south, and heavier in the east than in the west. These findings Land 2025, 14, 386 15 of 19

are consistent with the spatial distribution patterns of grassland degradation research hotspots in China over the past 20 years found by Hu et al. [48] We found that, at the global scale, changes in rural population size, changes in livestock numbers, changes in average temperature during the growing season, changes in maximum temperature during the growing period, and distance from roads were the main drivers affecting grassland change in Inner Mongolia during 2015–2020. Our study portrays the grassland change drivers and their contribution rates in Inner Mongolia in a more detailed and precise manner, which is a significant improvement on the results of previous overly cursory analyses of grassland change drivers by Ma et al. [49], Deyin et al. [50] and Li et al. [51]

This study shows that there is spatial differentiation in the dominant driving factors of grassland evolution in different regions. Therefore, grassland degradation prevention and management policies should be tailored to grasslands in different habitat contexts. For example, in areas where changes in rural population are the dominant factor in grassland degradation, management strategies should be formulated for the rural population, such as upgrading the level of urbanization and reducing the rural population. In areas where changes in the number of livestock are the dominant degradation factor, the number of livestock should be reasonably controlled according to the carrying capacity of grassland livestock. For areas where road distance dominates degradation, the construction of fences around roads should be strengthened to reduce the impact of road activities on grasslands.

This study provided comprehensive insights into the pixel-level dominant factors influencing grassland degradation. By identifying the key drivers specific to different regions, the research offered a detailed understanding of how these factors vary spatially across Inner Mongolia. The results significantly contribute to the theoretical framework and data foundation needed for a more refined interpretation of the relationship between grassland health and its influencing factors. This granular approach underscores the complexity of grassland ecosystems, highlighting the necessity for targeted and region-specific policies to effectively manage and mitigate grassland degradation. This data-driven strategy promotes sustainable grassland management and contributes to the mitigation of grassland degradation.

5.2. Limitations and Outlook

There are uncertainties in this study regarding the underlying data, data model conversion, and spatial and temporal scales of analysis. According to the assessment of Turner et al. [52], MODIS NPP data are overestimated in low productivity areas such as grasslands. However, considering that the misestimation of grassland NPP by MODIS products is systematic, whereas this paper focuses on multi-year trends in NPP, the underestimation of the absolute value of MODIS NPP does not significantly affect the conclusions of this paper. Nonetheless, this systematic bias may introduce uncertainties when analyzing the driving mechanisms of NPP changes in specific regions, particularly in areas with inherently low productivity. Future studies should consider incorporating corrections or using complementary high-resolution datasets such as Landsat and Sentinel data to mitigate this potential impact.

The economic and social development data (e.g., GDP, primary industry output value, population, number of various types of livestock, etc.) used in this study are based on county-level administrative units. However, in the specific analysis process, the authors did the homogenization process based on the area of the administrative area, thus generating spatialized data. Undoubtedly, the process of transforming from statistical data in the form of two-dimensional tables to spatial data, due to the difference in spatialization models, will cause greater uncertainty in the analysis results and give rise to incomparability between

Land 2025, 14, 386 16 of 19

different results. Future research should explore more refined spatialization techniques or incorporate multiple data sources to enhance accuracy.

Beyond data uncertainties, the models used in this study have inherent limitations that should be acknowledged. SHAP, when calculating Shapley values, involves repeated computations for each feature, which can result in high computational complexity, especially when dealing with high-dimensional data and large sample sizes. This increased computational cost may lead to extended processing times, particularly in large datasets or high-dimensional feature spaces. Future research could explore optimizing algorithms or utilizing alternative methods, such as LIME, to enhance the efficiency of its application in large-scale datasets.

When analyzing the driving factors, this study only considered the impact of climate change and socioeconomic development throughout the year or the growing season over the six-year period (2015–2020). However, the specific effects of these drivers in different years and months were not analyzed, nor was the potential lag effect accounted for, where changes in socioeconomic or climatic factors may not immediately translate into variations in NPP. This lag can lead to underestimation or overestimation of certain causal relationships. Additionally, differences in the analyzed time period and its granularity, as well as the omission of lag effects, could affect the accuracy and credibility of the results. Moreover, cross-scale influences pose a challenge, as interactions between large-scale climatic patterns and local ecological responses may not be fully captured by models trained at a single spatial resolution. Future research could address these limitations by incorporating temporal dependencies, such as lagged predictor variables, and by integrating multi-scale modeling approaches to better capture hierarchical relationships in grassland ecosystems.

6. Conclusions

In this paper, the authors proposed a technical framework based on an interpretable ML method for the selection of key driving elements of grassland change, the determination of the contribution rate of driving factors, and the spatial mapping of dominant driving factors, and carried out a case application in Inner Mongolia, China. The study proves the effectiveness of using ML methods, SHAP methods, GIS and other methods to analyze and map the driving mechanisms of grassland evolution, which provides a scientific basis for the local government to manage grassland degradation and it also provides a reference for the study of the driving mechanisms of natural and ecological changes in similar regions.

The study shows that grassland degradation in Inner Mongolia has an obvious spatial distribution pattern, and the LightGBM model can achieve the best prediction results in terms of prediction accuracy, reliability and stability. Changes in rural population size, changes in livestock size, changes in average temperature during the growing season, changes in maximum temperature during the growing period, and distance from roads are the key elements driving changes in the Inner Mongolian grasslands. This study also completed spatial mapping of the dominant elements of grassland degradation, providing a scientific basis for designing geographically targeted grassland degradation management initiatives.

Future research could focus on addressing the limitations of this study, such as incorporating temporal dependencies and lag effects, exploring the scale effects of data with different resolutions, and investigating alternative interpretative models and methods. These improvements would enhance the model's ability to capture complex interactions within grassland ecosystems, providing more accurate predictions and deeper insights for sustainable management practices. Additionally, applying this framework to regions with different ecological characteristics would further validate its applicability and effectiveness in a broader context.

Land 2025, 14, 386 17 of 19

Author Contributions: Z.Z.: methodology, formal analysis and investigation, writing—original draft preparation, writing—review and editing, data collection, visualization. Y.H.: conceptualization, methodology, writing—review and editing, funding acquisition, supervision, project administration. B.: methodology, funding acquisition, writing—review and editing. All authors have read and agreed to the published version of the manuscript.

Funding: This study was supported by the National Natural Science Foundation of China (42371304); the National Key Research and Development Plan Program of China [2021YFD1300501]; the Key Project of Innovation LREIS (KPI011); the Natural Science Foundation of Inner Mongolia Autonomous Region, China (2022QN04002); and the Special Fund for Basic Research Business of Inner Mongolia Normal University (2022JBQN098).

Data Availability Statement: The data used in the study and the access to them are available in Table 1. The code used during the current study is available from the corresponding author upon reasonable request.

Conflicts of Interest: The authors declare no conflicts of interest.

References

- 1. Bardgett, R.D.; Bullock, J.M.; Lavorel, S.; Manning, P.; Schaffner, U.; Ostle, N.; Chomel, M.; Durigan, G.; Fry, E.L.; Johnson, D.; et al. Combatting global grassland degradation. *Nat. Rev. Earth Environ.* **2021**, 2, 720–735. [CrossRef]
- 2. Gang, C.; Zhou, W.; Chen, Y.; Wang, Z.; Sun, Z.; Li, J.; Qi, J.; Odeh, I. Quantitative assessment of the contributions of climate change and human activities on global grassland degradation. *Environ. Earth Sci.* **2014**, 72, 4273–4282. [CrossRef]
- 3. Bi, X.; Xu, X.; Zhang, L. Analysis of the Spatial-Temporal Evolution Patterns of Grassland Net Primary Productivity and Its Driving Mechanisms in the High-altitude Gradient Mountain-Basin System of Central Asia. *Ecol. Environ. Sci.* **2020**, *29*, 876–888.
- 4. Liu, Y.; Zhang, Z.; Tong, L.; Khalifa, M.; Wang, Q.; Gang, C.; Wang, Z.; Li, J.; Sun, Z. Assessing the effects of climate variation and human activities on grassland degradation and restoration across the globe. *Ecol. Indic.* **2019**, *106*, 105504. [CrossRef]
- 5. Chen, C.; Park, T.; Wang, X.; Piao, S.; Xu, B.; Chaturvedi, R.K.; Fuchs, R.; Brovkin, V.; Ciais, P.; Fensholt, R.; et al. China and India lead in greening of the world through land-use management. *Nat. Sustain.* **2019**, 2, 122–129. [CrossRef]
- 6. Harris, R.B. Rangeland degradation on the Qinghai-Tibetan plateau: A review of the evidence of its magnitude and causes. *J. Arid Environ.* **2010**, *74*, 1–12. [CrossRef]
- 7. Gao, Y.Z.; Giese, M.; Lin, S.; Sattelmacher, B.; Zhao, Y.; Brueck, H. Belowground net primary productivity and biomass allocation of a grassland in Inner Mongolia is affected by grazing intensity. *Plant Soil* **2008**, *307*, 41–50. [CrossRef]
- 8. van der Merwe, J.P.A.; Kellner, K. Soil disturbance and increase in species diversity during rehabilitation of degraded arid rangelands. *J. Arid. Environ.* **1999**, *41*, 323–333. [CrossRef]
- 9. Bi, X.; Li, B.; Zhang, L.; Nan, B.; Zhang, X.; Yang, Z. Response of grassland productivity to climate change and anthropogenic activities in arid regions of Central Asia. *PeerJ* **2020**, *8*, e9797. [CrossRef]
- 10. Chen, Y.Z.; Mu, S.J.; Sun, Z.G.; Gang, C.C.; Li, J.L.; Padarian, J.; Groisman, P.; Chen, J.P.; Li, S.W. Grassland Carbon Sequestration Ability in China: A New Perspective from Terrestrial Aridity Zones. *Rangel. Ecol. Manag.* **2016**, *69*, 84–94. [CrossRef]
- 11. Li, X.B.; Bai, Y.X.; Wen, W.Y.; Wang, H.; Li, R.H.; Li, G.Q.; Wang, H. Effects of grassland degradation and precipitation on carbon storage distributions in a semi-arid temperate grassland of Inner Mongolia, China. *Acta Oecologica-Int. J. Ecol.* **2017**, *85*, 44–52. [CrossRef]
- 12. Yan, R.; Gao, W.; Shen, B.; Zhang, Y.; Wang, M.; Zhu, X.; Xin, X. Index System for Quantitative Evaluation of Pasture Degradation in Meadow Grassland of Inner Mongolia. *Sci. Agric. Sin.* **2021**, *54*, 3343–3354.
- 13. Dashpurev, B.; Dorj, M.; Phan, T.N.; Bendix, J.; Lehnert, L.W. Estimating fractional vegetation cover and aboveground biomass for land degradation assessment in eastern Mongolia steppe: Combining ground vegetation data and remote sensing. *Int. J. Remote Sens.* **2023**, *44*, 452–468. [CrossRef]
- 14. Wang, Z.B.; Ma, Y.K.; Zhang, Y.N.; Shang, J.L. Review of Remote Sensing Applications in Grassland Monitoring. *Remote Sens.* **2022**, *14*, 2903. [CrossRef]
- 15. Furumi, S.; Ono, A.; Muramatsu, K.; Fujiwara, N. Estimation model of net primary production by vegetation for ADEOS-II/GLI data. In *Hyperspectral Remote Sensing of the Land and Atmosphere, Proceedings of the Second International Asia-Pacific Symposium on Remote Sensing of the Atmosphere, Environment, and Space, Sendai, Japan, 9–12 October 2000*; SPIE: Bellingham, WA, USA, 2001; pp. 205–213.
- 16. Gower, S.T.; Krankina, O.; Olson, R.J.; Apps, M.; Linder, S.; Wang, C. Net primary production and carbon allocation patterns of boreal forest ecosystems. *Ecol. Appl.* **2001**, *11*, 1395–1411. [CrossRef]

Land 2025, 14, 386 18 of 19

17. Zhu, L.Y.; Shi, M.M.; Fan, D.Q.; Tu, K.; Sun, W.B. Analysis of Changes in Vegetation Carbon Storage and Net Primary Productivity as Influenced by Land-Cover Change in Inner Mongolia, China. *Sustainability* **2023**, *15*, 4735. [CrossRef]

- 18. Potter, C.S.; Randerson, J.T.; Field, C.B.; Matson, P.A.; Vitousek, P.M.; Mooney, H.A.; Klooster, S.A. Terrestrial Ecosystem Production—A Process Model-Based on Global Satellite and Surface Data. *Glob. Biogeochem. Cycles* 1993, 7, 811–841. [CrossRef]
- 19. Tong, L.; Liu, Y.; Zhang, Z.; Li, X.; Wang, Q.; Li, J. Quantitative Assessment on the Relative Effects of Climate Variation and Human Activities on Grassland Dynamics in Northwest China. *Res. Soil Water Conserv.* **2020**, *27*, 202–210.
- 20. Wang, Z.Q.; Zhang, Y.Z.; Yang, Y.; Zhou, W.; Gang, C.C.; Zhang, Y.; Li, J.L.; An, R.; Wang, K.; Odeh, I.; et al. Quantitative assess the driving forces on the grassland degradation in the Qinghai-Tibet Plateau, in China. *Ecol. Inform.* **2016**, *33*, 32–44. [CrossRef]
- 21. Sun, C.Q.; Bao, Y.L.; Vandansambuu, B.; Bao, Y.H. Simulation and Prediction of Land Use/Cover Changes Based on CLUE-S and CA-Markov Models: A Case Study of a Typical Pastoral Area in Mongolia. *Sustainability* **2022**, *14*, 15707. [CrossRef]
- 22. Xu, M.R.; Zhang, J.; Li, Z.H.; Mo, Y. Attribution analysis and multi-scenario prediction of NDVI drivers in the Xilin Gol grassland, China. *J. Arid Land* **2022**, *14*, 941–961. [CrossRef]
- 23. Ge, W.; Deng, L.; Wang, F.; Han, J. Quantifying the contributions of human activities and climate change to vegetation net primary productivity dynamics in China from 2001 to 2016. *Sci. Total Environ.* **2021**, 773, 145648. [CrossRef] [PubMed]
- 24. Hua, Y.; Sa, R.; Wang, B. Spatial and temporal variation of grassland NPP and its driving forces in Inner Mongolia. *J. Desert Res.* **2021**, *41*, 130–139.
- 25. Hu, Y.; Daorina; Hu, Y. Vegetation Change and Driving Factors: Contribution Analysis in the Loess Plateau of China during 2000–2015. *Sustainability* **2019**, *11*, 1320. [CrossRef]
- 26. Huang, B.; Xie, C.; Tay, R. Support vector machines for urban growth modeling. GeoInformatica 2010, 14, 83–99. [CrossRef]
- 27. Tayyebi, A.; Pijanowski, B.C. Modeling multiple land use changes using ANN, CART and MARS: Comparing tradeoffs in goodness of fit and explanatory power of data mining tools. *Int. J. Appl. Earth Obs. Geoinf.* **2014**, *28*, 102–116. [CrossRef]
- 28. Ye, J.; Hu, Y.; Zhen, L.; Wang, H.; Zhang, Y. Analysis on Land-Use Change and Its Driving Mechanism in Xilingol, China, during 2000-2020 Using the Google Earth Engine. *Remote Sens.* **2021**, *13*, 5134. [CrossRef]
- 29. Lakes, T.; Müller, D.; Krüger, C. Cropland change in southern Romania: A comparison of logistic regressions and artificial neural networks. *Landsc. Ecol.* **2009**, 24, 1195–1206. [CrossRef]
- 30. Keneni, B.M.; Kaur, D.; Bataineh, A.A.; Devabhaktuni, V.K.; Javaid, A.Y.; Zaientz, J.D.; Marinier, R.P. Evolving Rule-Based Explainable Artificial Intelligence for Unmanned Aerial Vehicles. *IEEE Access* **2019**, 7, 17001–17016. [CrossRef]
- 31. Papadakis, E.; Adams, B.; Gao, S.; Martins, B.; Baryannis, G.; Ristea, A. Explainable artificial intelligence in the spatial domain (X-GeoAI). *Trans. GIS* **2022**, 26, 2413–2414. [CrossRef]
- 32. He, Z.Y.; Yang, Y.J.; Fang, R.Z.; Zhou, S.H.; Zhao, W.C.; Bai, Y.J.; Li, J.S.; Wang, B. Integration of shapley additive explanations with random forest model for quantitative precipitation estimation of mesoscale convective systems. *Front. Environ. Sci.* **2023**, 10, 1057081. [CrossRef]
- 33. Li, X.; Wu, C.; Meadows, M.E.; Zhang, Z.; Lin, X.; Zhang, Z.; Chi, Y.; Feng, M.; Li, E.; Hu, Y. Factors Underlying Spatiotemporal Variations in Atmospheric PM2.5 Concentrations in Zhejiang Province, China. *Remote Sens.* **2021**, *13*, 3011. [CrossRef]
- 34. Lyu, X.; Li, X.; Gong, J.; Wang, H.; Dang, D.; Dou, H.; Li, S.; Liu, S. Comprehensive Grassland Degradation Monitoring by Remote Sensing in Xilinhot, Inner Mongolia, China. *Sustainability* **2020**, *12*, 3682. [CrossRef]
- 35. Zhou, W.; Yang, H.; Huang, L.; Chen, C.; Lin, X.S.; Hu, Z.J.; Li, J.L. Grassland degradation remote sensing monitoring and driving factors quantitative assessment in China from 1982 to 2010. *Ecol. Indic.* **2017**, *83*, 303–313. [CrossRef]
- 36. Zhao, H.L.; Okuro, T.; Zhou, R.L.; Li, Y.L.; Zuo, X.A. Effects of grazing and climate change on sandy grassland ecosystems in Inner Mongolia. *Sci. Cold Arid Reg.* **2011**, *3*, 223–232.
- 37. Batunacun; Wieland, R.; Lakes, T.; Yunfeng, H.; Nendel, C. Identifying drivers of land degradation in Xilingol, China, between 1975 and 2015. *Land Use Policy* **2019**, *83*, 543–559. [CrossRef]
- 38. Farr, T.G.; Rosen, P.A.; Caro, E.; Crippen, R.; Duren, R.; Hensley, S.; Kobrick, M.; Paller, M.; Rodriguez, E.; Roth, L.; et al. The Shuttle Radar Topography Mission. *Rev. Geophys.* **2007**, *45*. [CrossRef]
- 39. Tatem, A.J. Comment: WorldPop, open data for spatial demography. Sci. Data 2017, 4, 170004. [CrossRef]
- 40. Mount, D.M.; Netanyahu, N.S. Computationally Efficient Algorithms for High-Dimensional Robust Estimators. *Cvgip-Graph. Models Image Process.* **1994**, *56*, 289–303. [CrossRef]
- 41. Breiman, L. Random Forests. Mach. Learn. 2001, 45, 5–32. [CrossRef]
- 42. Chen, Y.; Song, Y.; Wang, W. Grassland vegetation cover inversion model based on random forest regression: A case study in Burqin County, Altay, Xinjiang Uygur Autonomous Region. *Acta Ecol. Sin.* **2018**, *38*, 2384–2394.
- 43. Yu, H.; Wang, L.; Wang, Z.M.; Ren, C.Y.; Zhang, B. Using Landsat OLI and Random Forest to Assess Grassland Degradation with Aboveground Net Primary Production and Electrical Conductivity Data. *ISPRS Int. J. Geo-Inf.* **2019**, *8*, 511. [CrossRef]
- 44. Yan, H.; Ran, Q.W.; Hu, R.H.; Xue, K.; Zhang, B.A.; Zhou, S.T.; Zhang, Z.P.; Tang, L.; Che, R.X.; Pang, Z.; et al. Machine learning-based prediction for grassland degradation using geographic, meteorological, plant and microbial data. *Ecol. Indic.* **2022**, 137, 108738. [CrossRef]

Land 2025, 14, 386 19 of 19

45. Chen, T.; Guestrin, C. XGBoost: A Scalable Tree Boosting System. In Proceedings of the KDD '16: The 22nd ACM SIGKDD International Conference on Knowledge Discovery and Data Mining, San Francisco, CA, USA, 13–17 August 2016; pp. 785–794. [CrossRef]

- 46. Lundberg, S.M.; Lee, S.I. A Unified Approach to Interpreting Model Predictions. In Proceedings of the Advances in Neural Information Processing Systems 30 (NIPS 2017), Long Beach, CA, USA, 4–9 December 2017.
- 47. Lu, W.; Hu, Y.; Zhang, Z.; Cao, W. A dual-encoder U-Net for landslide detection using Sentinel-2 and DEM data. *Landslides* **2023**, 20, 1975–1987. [CrossRef]
- 48. Hu, Y.; Han, Y.; Zhang, Y.; Zhuang, Y. Extraction and Dynamic Spatial-Temporal Changes of Grassland Deterioration Research Hot Regions in China. *J. Resour. Ecol.* **2017**, *8*, 352–358.
- 49. Ma, M.; Zhang, S.; Wei, B. Temporal and Spatial Pattern of Grassland Degradation and Its Determinants for Recent 30 Years in Xilingol. *Chin. J. Grassl.* **2017**, *39*, 86–93.
- 50. Deyin, K.; Na, T.A.O.; Dasheng, Y.; Fuqiang, Z.; Xuebing, L.I. Study on Variation of Drought Index and Causes of Grassland Degradation in Bayannaoer Area. *Chin. J. Grassl.* **2007**, 29, 116–120.
- 51. Li, J.; Pan, H.; Wang, G. Degradation causes of typical steppe in Inner Mongolia. *Pratacultural Sci.* **2004**, 21, 49–51.
- 52. Turner, D.P.; Ritts, W.D.; Cohen, W.B.; Gower, S.T.; Running, S.W.; Zhao, M.S.; Costa, M.H.; Kirschbaum, A.A.; Ham, J.M.; Saleska, S.R.; et al. Evaluation of MODIS NPP and GPP products across multiple biomes. *Remote Sens. Environ.* 2006, 102, 282–292. [CrossRef]

Disclaimer/Publisher's Note: The statements, opinions and data contained in all publications are solely those of the individual author(s) and contributor(s) and not of MDPI and/or the editor(s). MDPI and/or the editor(s) disclaim responsibility for any injury to people or property resulting from any ideas, methods, instructions or products referred to in the content.